

EFFECT OF CYCLOSPORINE A ON THE KIDNEY OF RABBIT: A LIGHT AND ULTRASTRUCTURAL STUDY

Fathy Ahmed Fetouh, Abdelmonem Awad Hegazy*.

Department of Anatomy and Embryology, Faculty of Medicine, Zagazig University, Zagazig, Egypt.

ABSTRACT

Background: Nephrotoxicity is a relatively common problem in patients immunosuppressed with cyclosporine A (CsA) with an incidence reaching up to thirty percent. The present work aimed to study the histological and ultrastructural effects of CsA on the kidney of rabbit.

Materials and Methods: Two groups of Egyptian adult rabbits were used for this study (5 rabbits for each). One group was used as a control and the other group (experimental) was treated with CsA in a dose of 15 mg/kg of body weight for two weeks. The animals were anaesthetized; and kidney specimens were obtained, fixed and processed for light and electron microscopic examinations.

Results: CsA had adverse effects on the kidney especially renal corpuscles, proximal convoluted tubules, distal convoluted tubules and afferent glomerular arterioles. The renal corpuscles were observed with shrunken glomeruli, widening of Bowman's space and thickening of the Bowman's capsule. Also, there was obvious increase in mesangial cell number and overall glomerular obliteration due to large lining endothelial cells and encroachment of the mesangial cell matrix onto the capillary lumen. The renal tubules showed vacuolization and PAS positive inclusion bodies. The cells showed disordered brush border of microvilli. Many fibrocytes appeared inbetween the tubules. Peritubular capillary congestion was observed with an increase in the surrounding connective tissue. Ultrastructurally, the proximal convoluted tubules showed thick basement membrane with loss of the basal infolding. The mitochondria appeared degenerated with damaged transverse cristae. Electron dense lysosomes were seen in the cytoplasm. In distal convoluted tubules, the cells showed degenerated mitochondria and pyknotic nuclei. The afferent glomerular arterioles appeared with hyperplasia of juxtaglomerular cells that contained massive renin granules. The lining endothelial cells appeared protruding their nuclei into the lumen due to contraction of the smooth muscles.

Conclusions: It could be concluded that CsA had adverse structural changes on the kidney mainly on the nephron; renal corpuscles, proximal convoluted tubules, distal convoluted tubules and afferent glomerular arterioles. Defective renal function should always be a concern in the management of CsA treated patient.

KEYWORDS: Kidney, Cyclosporine A, Nephrotoxicity, Histology, Ultrastructure.

Address for Correspondence: Dr. Abdelmonem Hegazy (M.D.), Associate Professor, Anatomy and Embryology Department, Faculty of Medicine, Zagazig University, Zagazig 44519, Egypt.

E-Mail: dr.abdelmonemhegazy@yahoo.com, ahegazy@zu.edu.eg

Access this Article online

Quick Response code



DOI: 10.16965/ijar.2014.545

Web site: International Journal of Anatomy and Research
ISSN 2321-4287
www.ijmhr.org/ijar.htm

Received: 24 Nov 2014

Peer Review: 24 Nov 2014 Published (O):31 Dec 2014

Accepted: 09 Dec 2014 Published (P):31 Dec 2014

INTRODUCTION

Since its introduction in 1976, cyclosporine A (CsA) has markedly improved the survival of solid transplants and has also been beneficial for the treatment of autoimmune diseases [1]. Cyclo-

sporine A, a neutral lipophilic cyclic undecapeptide isolated from the fungus *Tolypocladium inflatum* gams. This molecule exerted a rather wide spectrum of biologic activities, including antiparasitic, fungicidal and

anti-inflammatory effects. It was subsequently discovered to be a powerful immunosuppressive agent [2]. The immunosuppressive properties of CsA allowed its utilization in several diseases such as uveitis, rheumatoid arthritis, nephrotic syndromes and others [3, 4]. However, the benefits of cyclosporine A therapy have been potentially offset by the occurrence of nephrotoxicity. CsA nephrotoxicity which has been reported since the early 1980s occurs even when low doses of the drug are used in the treatment of autoimmune diseases [1]. Also, in the setting of cardiac transplantation, CsA nephrotoxicity has been related to the development of end-stage renal failure in about 10 % of patients [5]. CsA nephrotoxicity is classified into two major categories: functional and structural. The functional is the consequence of vasoconstriction of the afferent arteriole, the structural lesion, affecting the afferent arteriole, glomerulus and tubule-interstitium [6]. Acute CsA nephrotoxicity occurs early after initiation of therapy and presents clinically with a transient elevation of the serum creatinine and arterial hypertension in the majority of cases [7]. Experimental research on CsA nephrotoxicity in rabbit is far less frequent than in the rat [8]. One study in New Zealand rabbits revealed morphological changes similar to those seen in man [9]. The present work aimed to study toxic effects of cyclosporine A on the structures of the kidney under light and electron microscopic investigation in rabbit.

MATERIALS AND METHODS

Animals: Ten adult male Egyptian (Gabali) rabbits weighing 1.5-2 kg were used in this study. The animals were maintained in cages with food and water ad libitum under controlled conditions of light, humidity and temperature. They were obtained from Animal House Colony of Faculty of Medicine, Zagazig University. All experimental procedures were conducted in accordance with the guide for the care and use of laboratory animals and in accordance with the local Animal Care and Use Committee.

Chemicals: Cyclosporine A used in the present study was in the form of oral solution (Sandimmun Neoral 100 mg/ml) and given to the animals in a distilled water by gavage using

sterile equipments. CsA was administered in a dose of 15 mg/kg of body weight for 2 weeks according to Rezzani [10] who stated that daily administration of CsA ranging from 15 to 25mg/kg was well tolerated and showed immunosuppressive effects like those observed in transplant patients; and also found that chronic CsA nephrotoxicity occurs as early as 2 weeks after treatment.

Experimental design: The rabbits were divided into two groups (five rabbits for each) and treated as follows: the first group served as control group and received distilled water; the second group animal (CsA-treated rabbits) were daily administered 15 mg/kg of body weight for 2 weeks. 24 hours after the last dose, the animals were anaesthetized by intra-abdominal injection of thiopental. A midline abdominal incision was performed and the kidneys were dissected out and processed for light and electron microscopic examination.

For light microscopic examination, the kidneys were fixed in 10% neutral formal-saline for 24 hours and were processed to prepare 5 micron thick paraffin sections. Paraffin sections were stained with periodic-acid Schiff (PAS) which stains basal lamina and the brush border of the proximal convoluted tubules and also positive for the granules of the juxtaglomerular cells [11,12] and the cytoplasmic lysosome-protein bodies in the proximal convoluted tubules [13]. Also, the sections were stained with Masson trichrome which stains the brush border (green) [14].

For electron microscopic examination, the cortex was cut into small pieces and immediately fixed in 2.5% glutaraldehyde buffered with 0.1M phosphate buffer at PH 7.4 for 2 hours at 4C° and then washed with the phosphate buffer, post-fixed in 1% osmium tetroxide in the same buffer for one hour at 4 C°. After washing in phosphate buffer, specimens were dehydrated with ascending grades of ethanol and then were put in propylene oxide for 30 minutes at room temperature, impregnated in a mixture of propylene oxide and resin (1:1) for 24 hours and in a pure resin for another 24 hours. Then, the specimens were embedded in Embed-812 resin in BEEM capsules at 60C° for 24 hours. Semi-thin sections of about one micron thick were

obtained by glass knives and stained with 1% toluidine blue and examined by light microscopy. Ultrathin sections of about 50-70nm thick were cut using diamond knives and mounted on a copper grids, stained with uranyl acetate and lead citrate [15,16].

The sections were examined using a JEOL JEM 1010 transmission electron microscope in Histology Department, Faculty of Medicine, Zagazig University and also, SEO model PEM transmission electron microscope in Military Medical Academy.

RESULTS

In control animals, the renal cortex examined by the light microscopy showed renal corpuscles, proximal convoluted tubules, distal convoluted tubules and afferent arterioles. The proximal tubules had large cuboidal cells with large round nuclei and prominent nucleoli. The lumen was filled with brush border formed by microvilli. The distal tubules had a wide lumen due to absence of the brush border (Figs. 1-5). The afferent arterioles appeared near the renal corpuscles with juxtaglomerular cells in their walls (Figs. 4,5).

By electron microscopic examination, the cells of proximal convoluted tubules showed numerous basal infoldings which were seen extending into the cytoplasm with intervening mitochondria. The mitochondria were found numerous, elongated and distributed all over the cytoplasm, mostly at the base. Some vesicles were seen near the apex. The nucleus was oval and regular in shape. The apical border showed an extensive amount of microvilli (Fig. 6). The distal convoluted tubules showed numerous mitochondria and the lumen showed scanty microvilli (Fig. 7). The renal corpuscles showed glomerular capillaries, podocytes and mesangial cells. The capillaries appeared with wide lumens containing red blood cells. The podocytes appeared near the capillaries with their pedicles (processes) grasping the capillaries. The mesangial cells were seen in-between the capillary lumens (Figs. 8-10). The afferent arteriole appeared with its lumen containing red blood cells and lined by endothelial cells.

An internal elastic lamina appeared above the endothelial cells followed by smooth muscle cells (Fig. 11).

In treated animals with CsA, light microscopy examination showed the proximal convoluted tubules, distal convoluted tubules, renal corpuscles, and afferent arterioles. The renal tubules showed vacuolization and PAS positive inclusion bodies. The nuclei of the lining epithelial cells of the proximal convoluted tubules were generally reduced in size and some appeared pyknotic. The cells showed disordered brush border of microvilli. Many fibrocytes appeared in-between the tubules. Peritubular capillary congestion was observed with increase of the surrounding connective tissue formation (Fig.12-15). The renal corpuscles were observed with shrunken glomeruli, widening of Bowman's space and thickening of the Bowman's capsule (Fig. 14). The afferent glomerular arterioles appeared with hyperplasia of juxtaglomerular cells that contained massive renin granules (Figs. 15,16).

By electron microscopic examination, the cells of the proximal convoluted tubules showed thick basement membrane with loss of basal infolding and decrease in number of mitochondria. The mitochondria appeared degenerated with damaged transverse cristae. Electron dense lysosomes were seen in the cytoplasm. Numerous and large vacuoles appeared near the apex (Fig. 17). In distal convoluted tubules, the cells showed degenerated mitochondria and pyknotic nuclei. In some cells, the damaged mitochondria appeared in addition to normal mitochondria. The damaged mitochondria appeared swollen and even some appeared vacuolated (Figs. 18,19). The renal corpuscles were observed with evident increase in mesangial cell number that were seen interposed between the capillaries and podocytes. There was an overall glomerular obliteration due to large lining endothelial cells and encroachment of the mesangial cell matrix onto the capillary lumen. Thick basement membrane of the capillary was observed (Figs. 20,21). The afferent arteriole was observed with lining endothelial cells that appeared protruding their nuclei into the lumen due to contraction of the smooth muscles (Fig. 22).

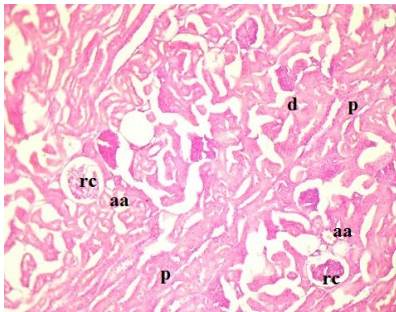


Fig. 1: A photomicrograph of a section in the renal cortex of control rabbit showing normal kidney structures; proximal convoluted tubules (p), distal convoluted tubules (d), renal corpuscles (rc) and afferent arteriole (aa). (PAS X 200).

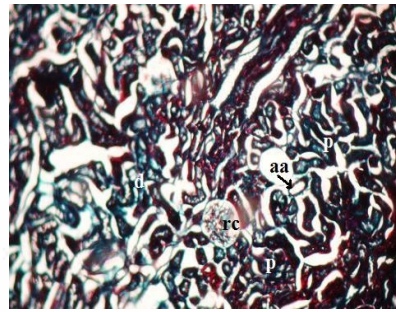


Fig. 2: A photomicrograph of a section in the renal cortex of control rabbit showing normal kidney structures; the proximal convoluted tubules (p) appear in longitudinal and cross sections with luminal brush border (green color), renal corpuscles (rc) and afferent arteriole (aa). (Masson trichrome X200).

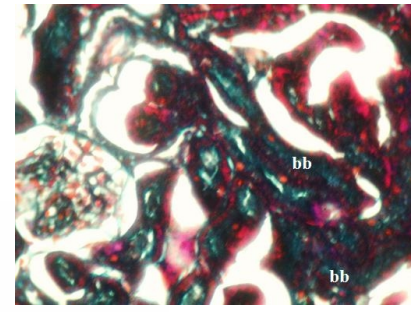


Fig. 3: A photomicrograph of a section with higher magnification in the renal cortex of control rabbit showing the proximal convoluted tubules with their epithelial cells are covered with a brush border (bb) of dense microvilli (stained green). (Masson trichrome X400).

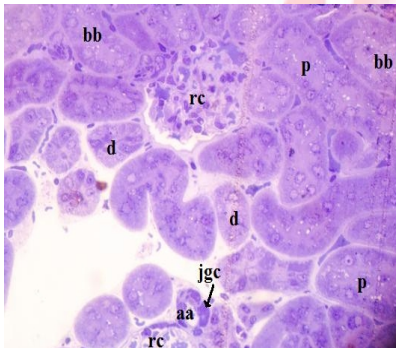


Fig. 4: A photomicrograph of a semi-thin section in the renal cortex of control rabbit. It shows renal corpuscles (rc), proximal (P) and distal (d) convoluted tubules. The proximal tubules have large cuboidal cells with large round nuclei and prominent nucleoli. The lumen is filled with the brush border (bb) formed by the microvilli. Afferent arterioles (aa) appear near the corpuscles with juxtaglomerular cells (jgc) in their walls. (Toluidine blue X400).

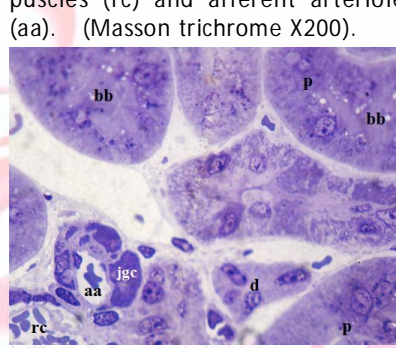


Fig. 5: A photomicrograph of a higher magnification of the previous figure. It shows part of renal corpuscles (rc), proximal (p) and distal (d) convoluted tubules. The proximal tubules have large cuboidal cells with large round nuclei and prominent nucleoli. The lumen is filled with the brush border (bb) formed by the microvilli. Afferent arteriole (aa) appears near by the corpuscle with juxtaglomerular cells (jgc) in their walls. (Toluidine blue X1000).

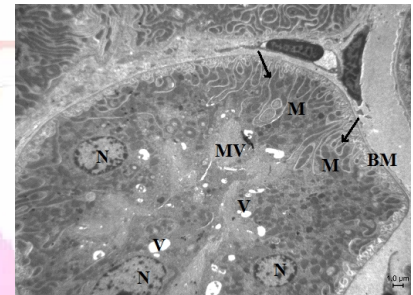


Fig. 6: An electron photomicrograph of ultrathin section in the renal cortex of control rabbit showing part of the proximal convoluted tubule in a transverse section. Numerous basal infoldings (arrows) are seen extending into the cytoplasm with intervening mitochondria (M). The mitochondria appear numerous, elongated and distributed mostly at the base. Some vesicles (V) are seen near the apex. The nucleus (N) is oval and regular in shape. The apical border shows extensive amount of microvilli (MV). (X 3000).

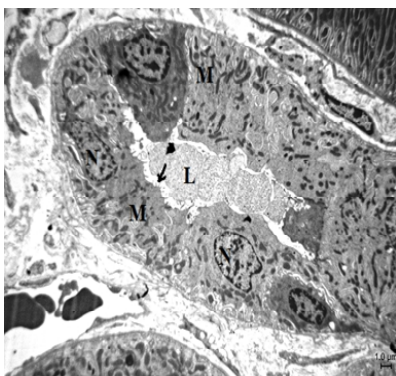


Fig. 7: An electron photomicrograph of ultrathin section in the renal cortex of control rabbit showing distal convoluted tubule in a transverse section. The lining cells show numerous mitochondria (M). The lumen (L) shows scanty microvilli (arrow). (X 3000).

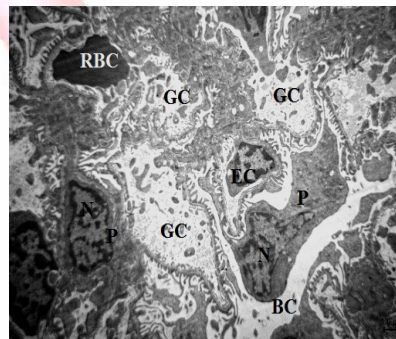


Fig. 8: An electron photomicrograph of ultrathin section in the renal cortex of control rabbit showing part of renal corpuscle where the glomerular capillaries (GC) appear lined by endothelial cell (EC) and contain red blood cells (RBC). 2 podocytes (P) with their nuclei (N) appear extending their processes into the neighboring capillaries in one side and related to the Bowman's space (BC) at the other side. (x 4000)

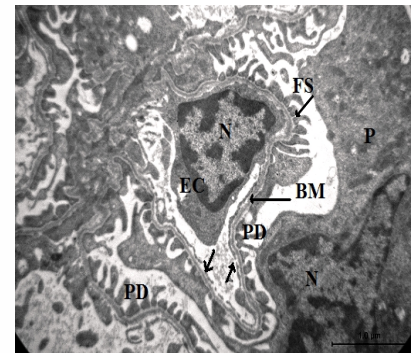


Fig. 9: An electron photomicrograph of a higher magnification of the previous figure showing one podocyte (P) extending pedicles (PD) to the outer surface of the glomerular capillary. Filtration slits (FS) appear in-between the pedicles. The glomerular capillary shows the basement membrane (BM) lined by fenestrated endothelium (arrows). (x 10000)

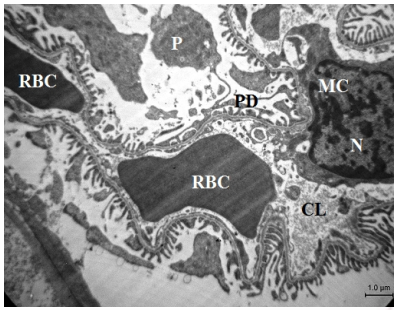


Fig. 10: An electron photomicrograph of another higher magnification showing one mesangial cell (MC) in-between 2 capillary lumens (CL). The capillary lumen appears wide and contains red blood cells (RBC) with pedicles (PD) of podocyte (P) reaching to the capillary. (x 8000)

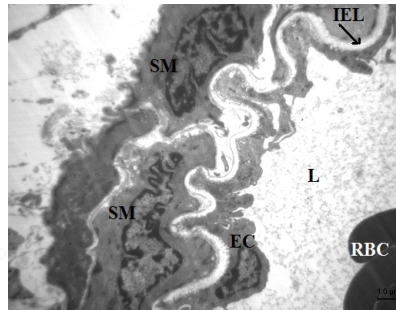


Fig. 11: An electron photomicrograph of ultrathin section in the renal cortex of control rabbit showing part of the wall in afferent arteriole. The lumen (L) contains red blood cells (RBC) and lined by endothelial cell (EC). An internal elastic lamina (IEL) appears above the endothelial cell followed by smooth muscle cells (SM). (x 6000)

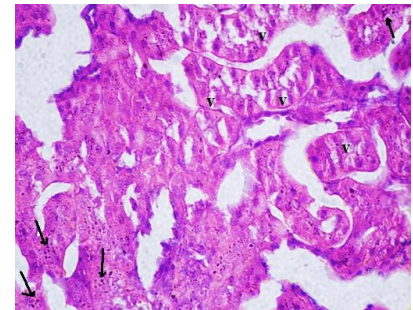


Fig. 12: A photomicrograph of a section in the renal cortex of CsA treated rabbit. The renal tubules show vacuolization (v) and PAS positive inclusion bodies (arrows). (PAS X 400)

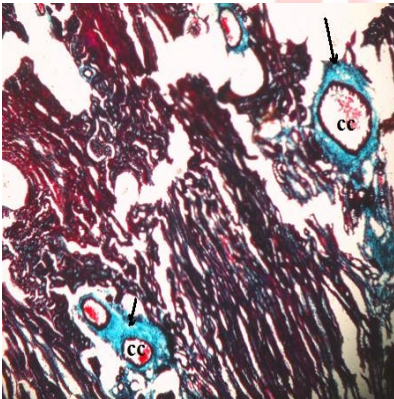


Fig. 13: A photomicrograph of a section in the renal cortex of CsA treated rabbit showing peritubular capillary congestion (cc) and increase in the surrounding connective tissue formation (arrows). (Masson trichrome X200)

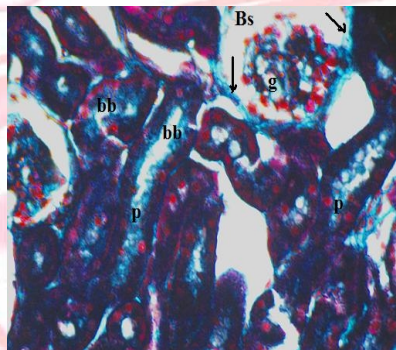


Fig. 14: A photomicrograph of a section in the renal cortex of CsA treated rabbit showing the proximal convoluted tubules (P) with disordered brush border (bb) of microvilli (stained green). The renal corpuscles contain shrunken glomeruli (g) with widening of the Bowman's space (Bs) and thickening of Bowman's capsule (arrow). (Masson trichrome X400)

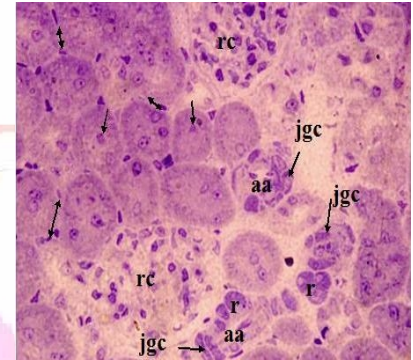


Fig. 15: A photomicrograph of a semi-thin section in the renal cortex of CsA treated rabbit showing renal corpuscles (rc) with reduced capillary lumens of the glomerulus. The nuclei of the lining epithelial cells of the proximal tubules are generally reduced in size and some appear pyknotic (arrow). Many fibrocytes (double headed arrows) appear in-between the tubules. Afferent glomerular arterioles (aa) appear with narrow lumens and hyperplasia of juxtaglomerular cells (jgc) with renin granules (r) in their walls are seen. (Toluidine blue X400)

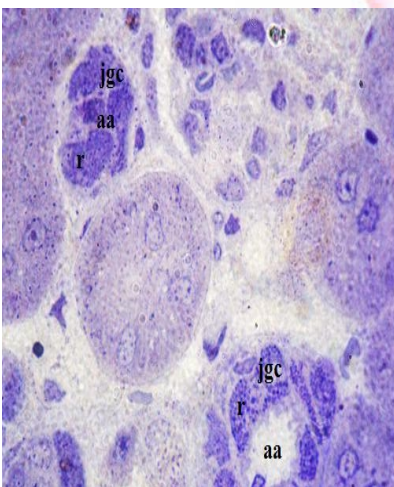


Fig. 16: A photomicrograph of a higher magnification of a semi-thin section in the renal cortex of CsA treated rabbit. Afferent glomerular arterioles (aa) appear with hyperplasia of juxtaglomerular cells (jgc) containing massive renin granules (r) in their walls. (Toluidine blue X1000)

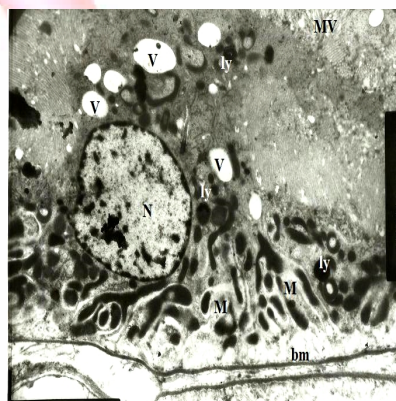


Fig. 17: An electron photomicrograph of ultrathin section in the renal cortex of CsA treated rabbit showing one of the epithelial cells of the proximal convoluted tubule. The cell shows thick basement membrane (bm) with loss of the basal infoldings with decrease in the number of mitochondria. The mitochondria (M) appear degenerated with damaged transverse cristae. Electron-dense lysosomes (ly) are seen in the cytoplasm. Numerous and large vacuoles (v) appear near the apex. (X 9000)

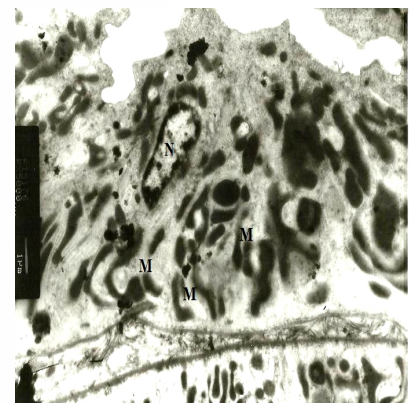


Fig. 18: An electron photomicrograph of ultrathin section in the renal cortex of CsA treated rabbit showing one of the epithelial cells of the distal convoluted tubule. The cell shows degenerated mitochondria (M) and pyknotic nucleus (N). (X 12000)

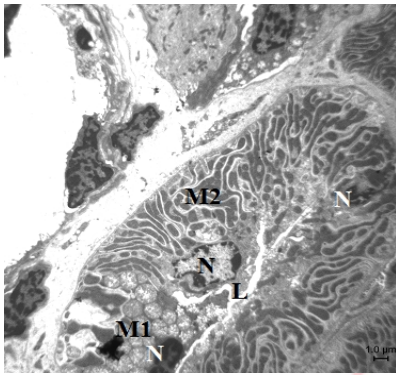


Fig. 19: An electron photomicrograph of ultrathin section in the renal cortex of CsA treated rabbit showing distal convoluted tubule with its lumen (L) in a transverse section. The lining cells show damaged mitochondria (M1) in addition to normal mitochondria (M2). The damaged mitochondria are swollen with loss of transverse cristae and even some appear vacuolated. Two of the nuclei (N) appear irregular and pyknotic. ($\times 3000$)

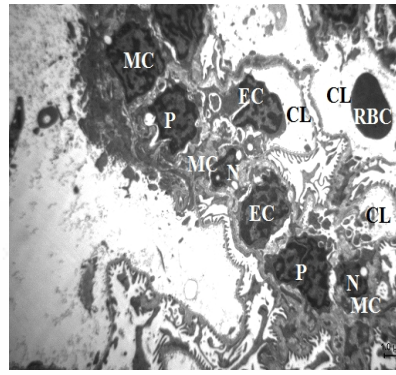


Fig. 20: An electron photomicrograph of ultrathin section in the renal cortex of CsA treated rabbit showing part of renal corpuscle where there is an evident increase in mesangial cell number (MC) interposed between the capillaries and the podocytes (P). There is an overall glomerular obliteration due to narrowing of the capillary lumen (CL), large lining endothelial cells (EC) and encroachment of the mesangial cells. The nuclei (N) are heterochromatic and darkly stained. ($\times 4000$)

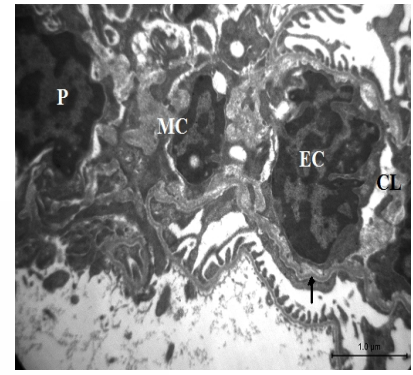


Fig. 21: An electron photomicrograph of a higher magnification of the previous figure showing one mesangial cell (MC) and surrounding matrix encroaching onto the nearby capillary lumen (CL). The capillary lumen appears narrow with large lining endothelial cell (EC) and thick basement membrane (arrow). ($\times 10000$)

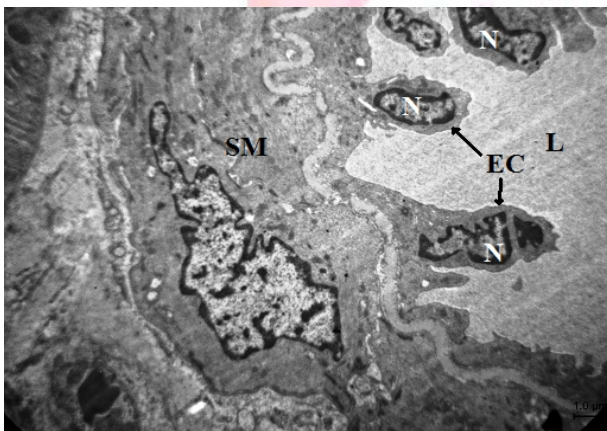


Fig. 22: An electron photomicrograph of ultrathin section in the renal cortex of CsA treated rabbit showing part of the wall of afferent arteriole surrounding a lumen (L). The lining endothelial cells (EC) appear protracting their nuclei (N) into the lumen due to contraction of the smooth muscles (SM). ($\times 6000$)

DISCUSSION

In the present study, treatment with CsA adversely affected the structure of the kidney mainly the tubular epithelium, renal corpuscles, and afferent arterioles. The proximal convoluted tubules revealed vacuolization and PAS positive inclusion bodies and some nuclei appeared pyknotic with disordered brush border of microvilli. Ultrastructurally, thick basement membrane with loss of basal infolding was observed and the mitochondria appeared degenerated with damaged transverse cristae. In addition, electron dense lysosomes were seen

in the cytoplasm. This is in accordance with Rezzani [10], and Pour et al. [17] who observed acute tubular changes in the form of loss of brush borders, presence of inclusion bodies and isometric vacuolization, which are usually observed in proximal tubules as early as 4 days after treatment with CsA. Alden and Frith [18] found that vacuolization may represent an initial stage preceding cell degeneration. Also, Abdel Fattah et al. [19] found that, CsA treated group showed renal tubules with vacuolated cytoplasm and others with darkly stained pyknotic nuclei. Apical brush borders of proximal tubules were undefined and PAS positive granules were noticed in their cytoplasm. Clarke and Ryan [20] found that the proximal tubular epithelia of CsA-treated animals were seen to have considerable damage to the mitochondria, including swelling and rounding of these organelles with dissolution of their cristae. There were increased levels of vacuolization with vacuoles of various sizes being present in CsA treated cells. Damage to the brush border of the cells was widely observed. Structurally, Owen [21] investigated the intracytoplasmic inclusions and suggested that they may represent myeloid bodies, giant mitochondria, or proliferation of smooth endoplasmic reticulum, usually involving the epithelium of proximal tubules. Also, Dell'Antonio and Randhawa [22]

found that, the inclusion bodies in the tubular cells were corresponding to giant mitochondria and microcalcification. In chronic CsA treatment, Agnieszka et al. [23] found that tubular epithelium cells revealed dilatation of endoplasmic reticulum, injury to mitochondria, formation of autolysosomes and presence of single apoptotic cells.

In the present study, many fibrocytes appeared in-between the tubules. Peritubular capillary congestion was observed with increase of surrounding connective tissue formation. This is in agreement with Rezzani [10] who mentioned that chronic CsA nephrotoxicity leads to interstitial fibrosis, tubular atrophy, and arteriolar hyalinosis. Ghiggeri et al. [24] found that very low concentration of CsA induced collagen synthesis in a variety of cultured human and rat renal fibroblasts. Also, Abdel Fattah et al. [19] found that inflammatory cellular infiltrate with increase in the collagen fibers were observed between the renal tubules. Many authors explained the increased fibrosis in CsA treatment. Johnson et al. [25] found that in vitro experiments with renal resident cells derived from rodents, primates and humans have shown that, CsA stimulates the production of collagen. Paul and de Fijter [26] found that CsA exerts renal tubular toxicity by local induction of vasoactive and chemotactic mediators that are secreted towards the baso-lateral compartment where they may induce interstitial inflammation and fibrosis. On the other hand, CsA may directly damage renal cells and induces cell death and subsequent fibrosis [27,28]

In the present study, the renal corpuscles were observed with shrunken glomeruli, widening of Bowman's space and thickening of Bowman's capsule. Ultrastructurally, there was an overall glomerular obliteration which was mostly due to large lining endothelial cells and encroachment of the mesangial cell matrix onto the capillary lumen. Thick basement membrane of the capillaries was observed. This is in agreement with Abdel Fattah et al. [19] who found that in CsA treated group, the renal corpuscles contained shrunken glomeruli with widening of their Bowman's space. Also, Ghiggeri et al. [24] found that CsA increases collagen synthesis in a variety of cultured human

and rat renal mesangial cells, Rezzani [10] observed focal glomerular scarring in chronic CsA nephrotoxicity.

In the present study, the afferent glomerular arterioles appeared with hyperplasia of juxtaglomerular cells that contained a massive amount of renin granules. Ultrastructurally, the afferent arteriole was observed with lining endothelial cells that appeared protruding their nuclei into the lumen due to contraction of the smooth muscles. This is in accordance with other authors who observed that CsA treatment results in extreme hyperplasia of the juxtaglomerular cells along the afferent arterioles [26,29]. Also, many researchers have shown a change in vascular flow with a decrease diameter of the afferent arteriole and progressive narrowing with CsA treatment [30-32]. CsA is capable of inducing a strong vasoconstriction in the afferent arteriole [30], which is mainly mediated by a rise in angiotensins secretion [33] and this would be the main mechanism of CsA induced nephrotoxicity [34,35].

The true aetiology of acute arterial effects has yet to be clearly established. It is thought to be multifactorial, resulting from a combination of an increase in vasoconstrictive factors (endothelin and thromboxane), activation of the renin-angiotensin-aldosterone system (RAAS), reduction of vasodilator factors (nitric oxide and prostacycline), and formation of free radicals [32,36,37]. Activation of RAAS system with calcineurin inhibitors involves both direct and indirect mechanisms. Directly, calcineurin inhibitors can activate juxtaglomerular cells to release renin. Indirectly, they can cause renin release from decreased perfusion as a result of arteriolar vasoconstriction [36-38].

Radical oxygen species (ROS) and lipid peroxidation have been involved in CsA induced nephrotoxicity by many researchers. CsA therapy causes dose and time related deterioration of kidney functions. The mechanism of effect is associated with increase in ROS, thromboxane secretion and also decrease of glomerular filtration rate with ROS, thromboxane and lipid peroxidates over production [39,40]. CsA administration induced significant elevation in lipid peroxidation along

with elevation in lipid peroxidation along with significant decrease in antioxidant enzyme activities, non enzymatic antioxidant, total antioxidant capacity and nitric oxide level in the rat kidney [41,42]. Also, treatment with CsA was found to significantly reduce plasma concentrations of adrenocorticotrophic hormone (ACTH), cortisol, and noradrenaline [43].

CONCLUSION

It could be concluded that CsA had adverse structural effects on the kidney mainly on the nephron; renal corpuscles, proximal convoluted tubules, distal convoluted tubules and afferent glomerular arterioles. Defective renal function should always be a concern in the management of CsA treated patient. Further studies are needed to clarify more about the exact mechanisms of CsA nephrotoxicity.

Acknowledgments

No funding was provided. We acknowledge Scientific and medical research center 'ZSMRC' of Zagazig Faculty of Medicine for its support.

Conflicts of Interests: None

REFERENCES

- [1]. Sund S, Forre O, Berg KJ, Kvien TK, Hovig T. Morphological and functional renal effects of long-term low-dose cyclosporin A treatment in patients with rheumatoid arthritis. *Clin Nephrol.* 1994;41:33-40.
- [2]. Borel JF, Feurer C, Gubler HU, Stahelin H. Biological effects of CsA: a new antilymphocytic agent. *Agents Action* 1976; 6: 468- 475.
- [3]. Bougneres PF, Carel JC, Castano L, Boitard C, Gardin JP, Landais P, Hors J, Mihatsch MJ, Paillard M, Chaussain JL, Bach JF. Factors associated with early remission of type I diabetes in children treated with cyclosporine. *New Engl J Med* 1988; 318: 663- 670.
- [4]. Durkan AM, Hodson EM, Willis NS, Craig JC. Immunosuppressive agents in childhood nephrotic syndrome: a meta-analysis of randomized controlled trails. *Kidney Int* 2001; 59: 1919- 1927.
- [5]. Goldstein DJ, Zuech N, Sehgal V. Cyclosporine-associated end-stage nephropathy after cardiac transplantation. *Transplantation* 1997;63: 664
- [6]. Bennett WM, Demattos A, Meyer MM, Andoh T, Barry JM. Chronic CsA nephropathy: The Achilles' heel of immunosuppressive therapy. *Kidney Int* 1996; 50:1089-1100.
- [7]. Morales JM, Andres A, Rengel M, Rodicio JL. Influence of cyclosporin, tacrolimus and rapamycin on renal function and arterial hypertension after renal transplantation. *Nephrol Dial Transplant* 2001;16 (1): 121-124.
- [8]. Thliveris JA, Yatscoff RW, Lukowski MP, Copeland KR. Cyclosporine nephrotoxicity-experimental models. *Clin Biochem* 1991a;24: 93-95.
- [9]. Thliveris JA, Yatscoff RW, Lukowski MP, Copeland KR, Jeffery JR, Murphy GF. Chronic cyclosporine nephrotoxicity: A rabbit model. *Nephron* 1991b;57: 470-476
- [10]. Rezzani R. Cyclosporine A and adverse effects on organs: histochemical studies. *Prog Histochem Cytochem* 2004; 39: 85-128.
- [11]. Thijssen S, Lambrichts I, Maringwa J, kerkhove EV. Changes in expression of fibrotic markers and histopathological alternations in kidneys of mice chronically exposed to low and high Cd doses. *Toxicol.*, 2007; 238: 200-210.
- [12]. Gartner PL, Hiatt J. *Color Atlas of Histology*, 3rd ed., Lippincott Williams and Wilkins, London, Sydney and Tokyo, 2000; pp: 327.
- [13]. Bancroft JD, Gamble M.: *Theory and Practice of Histological Techniques* 5th ed., Churchill Livingstone, New York, London, Philadelphia, 2002.
- [14]. Kuehnel W. *Color Atlas of Cytology, Histology and Microscopic Anatomy*, 4th ed., Thieme Flexibook, Stuttgart, New York, 2002, pp: 364 & 368.
- [15]. Bozzola JJ, Russell LD. *Electron microscopy principles and techniques for biologists*. Jones and Bartlett publisher, Boston, 1995.
- [16]. Glauert AM, Lewis PR. *Biological specimen preparation for transmission electron microscopy*. Vol 17, Portland press, London, 1998.
- [17]. Pour ZM, Vessal M, Zal F, Khoshdel Z, Torabinejad S. Protective effects of vitamin E and/or quercetin co-supplementation on the morphology of kidney in cyclosporine A- treated rats. *Iran J Med Sci* 2009; 34(4):271-276.
- [18]. Alden CL, Frith CH. Urinary system. In: Haschek WM, Rousseaux CG (eds). *Handbook of toxicologic pathology*. Academic Press, San Diego 1991, pp 315-387.
- [19]. Abdel Fattah EA, Hashem HE, Ahmed FA, Ghallab MA, Varga I, Polak S. Prophylactic role of curcumin against cyclosporine-induced nephrotoxicity: histological immunohistological study. *Gen Physiol Biophys* 2010; 29(1): 85-94.
- [20]. Clarke H, Ryan MP. Cyclosporine A-induced alterations in magnesium homiostasis in the rat. *Life Sciences* 1999; 64(15):1295-1306.
- [21]. Owen RA. Acute tubular lesions, kidney rat. In: Jones TC, Mohr U, Hunt RD (eds). *Monographs on pathology of laboratory animals. Urinary system*. Springer-Verlag, Berlin 1986, pp 229-238.
- [22]. Dell'Antonio G, Randhawa PS. Striped pattern of medullary ray fibrosis in allograft biopsies from kidney transplant recipients maintained on tacrolimus. *Transplantation* 1999; 67:484-486.
- [23]. Agnieszka K, Mariusz M, Grazyna C, Monika O. Ultrastructural examination of renal tubular epithelial cells and hepatocytes in the course of chronic cyclosporine A treatment-A possible link to oxidative stress. *Ultrastructural pathology* 2013;37(5):332-339.

- [24]. Ghiggeri GM, Altieri P, Oleggini R, Valenti F. Cyclosporine enhances the synthesis of selected extracellular matrix proteins by renal cells (in culture). Different cell responses and phenotype characterization. *Transplantation* 1994;57:1382-1388.
- [25]. Johnson DW, Saunders HJ, Johnson FJ. Cyclosporine exerts a direct fibrogenic effect on human tubulointerstitial cells: Roles of insulin-like growth factor 1, transforming growth factor beta 1, and platelet-derived growth factor. *J Pharmacol Exp Ther* 1999;289:535-542.
- [26]. Paul LC, de Fijter JH. Cyclosporine-induced renal dysfunction. *Transplant Proc* 2004;36 (2suppl): 224s-228s.
- [27]. Kahn GC, Shaw LM, Kane MD. Routine monitoring of cyclosporine in whole blood and in kidney tissue using high performance liquid chromatography. *J Anal Toxicol* 1986;10:28-34.
- [28]. Wang C, Salahudeen AK. Cyclosporine nephrotoxicity: attenuation by an antioxidant-inhibitor of lipid peroxidation in vitro and vivo. *Transplantation* 1994;58(8):940-946.
- [29]. Nitta K, Friedman AL, Nicastrì AD. Granular juxtaglomerular cell hyperplasia caused by cyclosporine. *Transplantation* 1987; 44:417- 421.
- [30]. English J, Evan A, Houghton DC. Cyclosporine-induced acute renal dysfunction in the rat. Evidence of arteriolar vasoconstriction with preservation of tubular function. *Transplantation* 1987;44 :135-141
- [31]. Laskow DA, Curtis JJ, Luke RG, Julian BA, Jones P. Cyclosporine- induced changes in glomerular filtration rate and urea excretion. *Am J Med.* 1990; 5(88): 497-502.
- [32]. Issa N, Kukla A, Ibrahim HN. Calcineurin inhibitor nephrotoxicity: a review and perspective of the evidence. *Am J Nephrol.* 2013; 37(6): 602-612.
- [33]. Bergamasco L, Sainaghi PP, Castello L, Letizia C, Bartoli E. In vitro effect of cyclosporine A on angiotensins secretion by glomerular cells. *Nephrology* 2008; 13:302-308.
- [34]. Ishikawa, Suzuki K, Fujita K. Mechanisms of cyclosporine-induced nephrotoxicity. *Transplant Proc* 1999;31:1127-1128.
- [35]. Bertani T, Ferrazzi P, Schieppati A. Nature and extend of glomerular injury induced by cyclosporine in heart transplant patient. *Kidney Int* 1991;40:243-250.
- [36]. Naesens M, Kuypers DR, Sarwal M. Calcineurin Inhibitor Nephrotoxicity. *Clin J Am Soc Nephrol.* 2009; 4:481-508.
- [37]. Bobadilla NA, Gamba G. New insights into the pathophysiology of cyclosporine nephrotoxicity: a role of aldosterone. *Am J Physiol Renal Physiol.* 2007; 293 (1):F2-9.
- [38]. Hoorn EJ, Walsh SB, Mc Cormick JA, Furstenberg A, Yang CL. The calcineurin inhibitor tacrolimus activates the renal sodium chloride transport to cause hypertension. *Nat Med.* 2011; 17(10): 1304-1309.
- [39]. Krauskopf A, Buetler TM, Nguyen NS, Mace K, Ruegg UT. Cyclosporin A-induced free radical generation is not mediated by cytochrome P-450. *Br J Pharmacol* 2002;135(4): 977-986.
- [40]. Galletti P, Di Gennaro CI, Migliardi V, Indaco S, Della RF, Manna C. Diverse effects of natural antioxidants on cyclosporine cytotoxicity in rat renal tubular cells. *Nephrol Dial Transplant* 2005;20(8):1551-1558.
- [41]. Hussein SA, Ragab OA, El-Eshrawy MA. Renoprotective effect of dietary fish oil on cyclosporine A: Induced nephrotoxicity in rats. *Asian Journal of Biochemistry* 2014;9:71-85.
- [42]. Ghaznavi R, Zahmatkesh M, Kadkhodae M, Mahdavi-Mazdeh M. Cyclosporine effects on the antioxidant capacity of rat renal tissues. *Transplant Proc* 2007;39:866-867.
- [43]. Antje Albring, Laura Wendt, Nino Harz, Engler H, Wilde B, Witzke O, Schedlowsk M. Short-term treatment with the calcineurin inhibitor cyclosporine A decreases HPA axis activity and plasma noradrenaline levels in healthy male volunteers. *Pharmacology Biochemistry and Behavior*, 2014; 126: 73–76.

How to cite this article:

Fetouh FA, Hegazy AA. EFFECT OF CYCLOSPORINE A ON THE KIDNEY OF RABBIT: A LIGHT AND ULTRASTRUCTURAL STUDY. *Int J Anat Res* 2014;2(4):768-776. DOI: 10.16965/ijar.2014.545